BIOCHEMISTRY
including biophysical chemistry & molecular biology

ARTICLE

pubs.acs.org/biochemistry

# Activated ERK2 Is a Monomer in Vitro with or without Divalent Cations and When Complexed to the Cytoplasmic Scaffold PEA-15

Tamer S. Kaoud,[†,§] Ashwini K. Devkota,[†,∥] Richard Harris,[⊥] Mitra S. Rana,[∥] Olga Abramczyk,[†] Mangalika Warthaka,[†] Sunbae Lee,[†] Mark E. Girvin,[⊥] Austen F. Riggs,[∥,‡] and Kevin N. Dalby*[,†,§,∥]

[†]Division of Medicinal Chemistry, University of Texas, Austin, Texas 78712, United States

[‡]Section of Neurobiology, School of Biological Sciences, University of Texas, Austin, Texas 78712, United States

[§]Graduate Program in Pharmacy and [∥]Graduate Program in Cell and Molecular Biology, University of Texas, Austin, Texas 78712, United States

[⊥]Biochemistry Department, Albert Einstein College of Medicine, 1300 Morris Park Avenue, Bronx, New York 10461, United States

**ABSTRACT:** The extracellular signal-regulated protein kinase, ERK2, fully activated by phosphorylation and without a $His_6$ tag, shows little tendency to dimerize with or without either calcium or magnesium ions when analyzed by light scattering or analytical ultracentrifugation. Light scattering shows that ~90% of ERK2 is monomeric. Sedimentation equilibrium data (obtained at 4.8−11.2 $\mu$M ERK2) with or without magnesium (10 mM) are well described by an ideal one-component model with a fitted molar mass of 40180 ± 240 Da (without $Mg^{2+}$ ions) or 41290 ± 330 Da (with $Mg^{2+}$ ions). These values, close to the sequence-derived mass of 41711 Da, indicate that no significant dimerization of ERK2 occurs in solution. Analysis of sedimentation velocity data for a 15 $\mu$M solution of ERK2 with an enhanced van Holde−Weischet method determined the sedimentation coefficient ($s$) to be ~3.22 S for activated ERK2 with or without 10 mM $MgCl_2$. The frictional coefficient ratio ($f/f_0$) of 1.28 calculated from the sedimentation velocity and equilibrium data is close to that expected for an ~42 kDa globular protein. The translational diffusion coefficient of ~$8.3 \times 10^{-7}$ $cm^2\ s^{-1}$ calculated from the experimentally determined molar mass and sedimentation coefficient agrees with the value determined by dynamic light scattering in the absence and presence of calcium or magnesium ions and a value determined by NMR spectrometry. ERK2 has been proposed to homodimerize and bind only to cytoplasmic but not nuclear proteins [Casar, B., et al. (2008) *Mol. Cell 31*, 708−721]. Our light scattering data show, however, that ERK2 forms a strong 1:1 complex of ~57 kDa with the cytoplasmic scaffold protein PEA-15. Thus, ERK2 binds PEA-15 as a monomer. Our data provide strong evidence that ERK2 is monomeric under physiological conditions. Analysis of the same ERK2 construct with the nonphysiological $His_6$ tag shows substantial dimerization under the same ionic conditions.

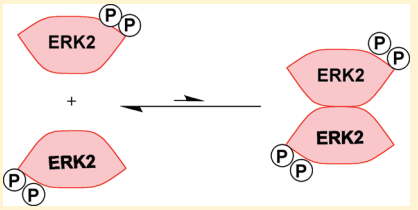


Mitogen-activated protein kinases (MAPKs) are pivotal enzymes in cellular communication and include the extracellular signal-regulated kinase family (ERKs), the c-Jun N-terminal kinase family (JNKs), and the p38MAP kinase family.[1] The ERKs mediate effects on proliferation and differentiation by growth factors and hormones. The JNKs and p38 MAPKs help fashion cellular responses to stress. Breakdown in the control of these enzymes can lead to numerous cancers and degenerative diseases.[2] MAPKs each have multiple protein substrates yet paradoxically elicit specific biological responses. An understanding of the rules governing the interactions between these kinases and other cellular proteins will provide insight into how this specificity is achieved and help in identifying strategies for correcting biological signals when they go awry.

The ERK1 and ERK2 pathway begins with Ras, a GTPase.[3] Ras is anchored to the cytoplasmic face of the plasma membrane and is activated by a cascade of events after various hormones bind to their respective cell surface receptors. Following activation, Ras recruits Ser/Thr-specific Raf kinases to the cellular membrane[4] and induces their activation through a series of complex phosphorylation events.[5,6] Phosphorylated Raf kinases then activate two closely related cytoplasmic kinases, MKK1 and MKK2, by phosphorylating each within its respective activation loop at Ser-217 and Ser-221.[7] Activated MKK1 and MKK2 can then activate ERK1 and ERK2 by phosphorylation.[8] Activated ERK1 and ERK2 are found in both the nucleus and cytoplasm, but only cytoplasmic ERK1 and ERK2 are likely to activate the Ser/Thr-specific RSK1 and RSK2 kinases,[9−12] which can then join nuclear ERK1 and ERK2 to phosphorylate transcriptional regulators that include Elk-1,[13] SAP1, and SAP2.[14] This transcriptional activation results in the rapid appearance of products of immediate early genes, which include transcription factors that control cell survival and/or the cell cycle.

X-ray crystallographic analysis of activated $His_6$-ERK2 revealed a putative dimeric interface facilitated by a nonhelical leucine zipper comprised of residues L333, L334, and L336 from

**Received:** February 9, 2011
**Revised:** April 20, 2011
**Published:** April 20, 2011

each monomer subunit.[15] Phosphorylated $His_6$-ERK2 and unphosphorylated $His_6$-ERK2 were reported to self-associate to form homodimers with dissociation constants of 7.5 and 20000 nM, respectively, in the absence of added divalent metal ions.[15] $His_6$-ERK2 has been reported to be monomeric in the presence of chelating agents, such as EDTA and EGTA,[16,17] and divalent metal ions such as $Mg^{2+}$ and $Ca^{2+}$ have been reported to be essential for dimerization.[16] In vivo studies failed to detect the presence of GFP-ERK2 homodimers in cells under conditions where GFP-ERK·GFP-MKK1 dimers were readily observed.[18] However, ERK2 was reported to associate as a homodimer into cytoplasmic scaffolds following cell stimulation, and it was proposed that this "assembly-mediated" dimerization in the cytoplasm is important for tumorigenesis.[19] In contrast, ERK2 was reported to associate with nuclear proteins only as a monomer.[19]

$His_6$ tags have been shown to promote the self-association of some proteins[20,21] and could potentially influence the tendency of ERK2 monomers to dimerize. For example, we have found that the presence of a $His_6$ tag at the N-terminus of p38 MAPK α dramatically improves its ability to be phosphorylated by MKK6.[22] Furthermore, transition metals such as nickel and cobalt bind $His_6$ tags[23] and if present in trace amounts could influence the properties of a protein. We reevaluated the self-association of activated ERK2 without the $His_6$ tag and also asked whether ERK2 self-associates on the cytoplasmic scaffold protein PEA-15. We find that activated ERK2 binds to PEA-15 as a monomer. These results suggest that activated ERK2 is predominantly monomeric.

## MATERIALS AND METHODS

**Materials.** Yeast extract, tryptone, and agar were purchased from U.S. Biological (Swampscott, MA). Competent cells used for amplification and expression were obtained from Novagen (Gibbstown, NJ). Ni-NTA Agarose, the QIAprep Spin Miniprep Kit, the QIAquick PCR Purification Kit, and the QIAquick Gel Extraction Kit were provided by Qiagen (Valencia, CA). Enzymes for restriction digestion and ligation were obtained from New England BioLabs (Ipswich, MA) and Invitrogen Corp. (Carlsbad, CA). respectively. All the buffer components used for protein purification and experimental procedures were obtained from Sigma (St. Louis, MO). Amersham Biosciences (Pittsburgh, PA) provided the FPLC system and the columns for purification. P81 cellulose papers were obtained from Whatman (Piscataway, NJ). ATP was purchased from Roche (Indianapolis, IN). Radiolabeled [$\gamma$-$^{32}$P]ATP was obtained from Perkin-Elmer (Waltham, MA).

**Protein Preparation.** *Construction of a $His_6$ Cleavable Construct of ERK2 in pET28a.* We previously constructed pET28-$His_6$-ERK2 Cysless PKA. A mutant of ERK2 lacking cysteines with a thrombin cleavable N-terminal $His_6$ tag and C-terminal PKA tag was cloned into a pET28a expression vector at the NdeI and HindIII restriction sites.[24] To generate a wild-type construct, a SacII−HindIII fragment containing all the mutations and the C-terminal PKA tag was replaced by DNA encoding wild-type ERK2 (*Rattus norvegicus* mitogen-activated protein kinase 1, GenBank accession number NM_053842).[24] The resulting construct contains a $His_6$ tag followed by a thrombin cleavage site (Met-Gly-Ser-Ser-His-His-His-His-His-His-Ser-Ser-Gly-Leu-Val-Pro-Arg-Gly-Ser-His) at the N-terminus of the ERK2 sequence immediately preceding Met-1. The sequence was verified at the Institute for Cell and Molecular Biology (ICMB) Sequencing Facility at the University of Texas.

*ERK2 Expression and Purification.* A pET28a-$His_6$-ERK2 plasmid with a cleavable $His_6$ tag was transformed into BL21-(DE3) cells. Cells from a single colony were used to inoculate 100 mL of LB medium containing 30 μg/mL kanamycin and grown overnight at 37 °C. The culture was diluted 100-fold into 4 L of LB broth containing 30 μg/mL kanamycin and was grown at 37 °C to an optical density of 0.6 at 600 nm. The cells were induced with 500 μM IPTG and cultured for an additional 4 h at 30 °C. The cells were harvested, flash-frozen in liquid nitrogen, and stored at −80 °C until they were lysed. Cells were lysed in 200 mL of buffer A [40 mM Tris (pH 7.0), 0.03% Brij-30, 0.1% β-mercaptoethanol, 1 mM benzamidine, 0.1 mM TPCK, and 0.1 mM PMSF] containing 750 mM NaCl, 5 mM imidazole, and 1% Triton X-100 and sonicated at 4 °C for 20 min using a 5 s pulse with 5 s intervals. The lysate was centrifuged (16000 rpm) at 4 °C for 30 min, and the supernatant was agitated gently with 10 mL of Ni-NTA beads (Qiagen) at 4 °C for 1 h. The beads were washed with 200 mL of buffer A containing 10 mM imidazole with the pH readjusted to 7.5 and then eluted with 50 mL of buffer A containing 200 mM imidazole with the pH readjusted to 8.0. An aliquot of the eluted protein, 50 mL, was loaded onto a Mono-Q HR 10/10 anion exchange column pre-equilibrated with buffer B [20 mM Tris (pH 8.0), 0.03% Brij-30, 0.1 mM EDTA, 0.1 mM EGTA, and 0.1% β-mercaptoethanol]. The protein was chromatographed in Mono-Q buffer with a gradient from 0 to 0.5 M NaCl over 17 column volumes (∼170 mL) and was eluted at ∼0.25 M NaCl. The eluted fractions of $His_6$-ERK2 were pooled and dialyzed overnight against either buffer S [25 mM HEPES (pH 7.5), 50 mM KCl, 0.1 mM EDTA, 0.1 mM EGTA, 2 mM DTT, and 10% glycerol] for further activation or thrombin cleavage buffer C [20 mM Tris-HCl (pH 8.3), 150 mM NaCl, 2.5 mM $CaCl_2$, and 0.1% β-mercaptoethanol] for further $His_6$ tag cleavage. Cleavage was performed at 23 °C for 5 h by mixing 1 unit of thrombin (Novagen) per milligram of ERK2. The cleavage was verified by electrophoresis via 10% sodium dodecyl sulfate−polyacrylamide gel electrophoresis (SDS−PAGE). After $His_6$ tag cleavage, the protein was dialyzed overnight against buffer B, filtered, and loaded on a Mono-Q HR 10/10 anion exchange column. The separation of tagless ERK2 from uncleaved protein or $His_6$ tag was accomplished as described above. Cleavage was confirmed by ESI-MS. Eluted fractions were pooled and dialyzed against buffer S for further activation.

*Activation of ERK2.* Either $His_6$-cleaved or $His_6$-tagged ERK2 (7 μM) was incubated with constitutively active MKK1 (0.35 μM) in buffer D [25 mM HEPES (pH 7.5), 0.1 mM EGTA, 20 mM $MgCl_2$, 2 mM DTT, and 4 mM ATP] to a 50 mL final volume at 27 °C for 6 h. The activated protein was dialyzed against Mono-Q buffer B (pH 8) and purified with a Mono-Q HR 10/10 anion exchange column as described above. The purity and identity of the active ERK2 were verified by running the protein fractions on 10% SDS−PAGE and by ESI-MS. Eluted fractions were pooled and dialyzed against buffer S and then concentrated using an Amicon Ultra-15 instrument (10000 molecular weight cutoff), frozen in liquid nitrogen, and stored at −80 °C. For analytical ultracentrifugation, the active tagless enzyme was further purified by HIC, diluted 10-fold in buffer E [50 mM potassium phosphate buffer (pH 7.4), 0.1 mM EDTA, 0.1 mM EGTA, 0.1% β-mercaptoethanol, and 1 M ammonium sulfate], and loaded onto a HiLoad 16/10 Phenyl Sepharose

High Performance column (2.6 cm × 10 cm) that was pre-equilibrated with buffer E. The column was run with a decreasing gradient concentration of ammonium sulfate from 1 to 0 M. The protein was eluted at ~0.2 M ammonium sulfate. Eluted fractions were pooled and dialyzed against buffer S. The purity of the protein was confirmed by SDS−PAGE. In all cases, the concentration of activated ERK2 was determined with an extinction coefficient ($A_{280}$) of 52067 $cm^{-1}$ $M^{-1}$.[24] The activation status of the protein was verified by ESI-MS performed at the Institute for Cell and Molecular Biology Mass Spectrometry Facility at the University of Texas and also by an in vitro kinase assay with *Ets* as a substrate.[25]

*Constitutively Active MKK1 and Ets Expression and Purification.* Expression and purification of MKK1 and *Ets* have been described previously.[25]

*Expression and Purification of Tagless Full-Length PEA-15.* Full-length PEA-15 was cloned into the pET28a vector[26] and transformed into BL21(DE3)-pLys cells. Cells were grown at 37 °C in Luria broth medium containing 30 μg/mL kanamycin to an optical density of 0.6 at 600 nm. Protein expression was induced with 0.5 mM IPTG, and the cells were cultured for an additional 4 h at 30 °C before being harvested. The purification of $His_6$-PEA-15 was similar to that of ERK2, except a 0 to 250 mM NaCl gradient was used for elution of PEA-15 from the Mono-Q HR 10/10 column (yield of ~65 mg/L of culture). $His_6$-PEA-15 (10 mg) was cleaved to tagless PEA-15 by thrombin in a 10 mL reaction volume containing 10 units of thrombin (Calbiochem). The cleavage was conducted for 5 h at 25 °C in buffer C. The resulting PEA-15 contains three residues, Gly-Ser-His, at the N-terminus before Met-1. The reaction sample (10 mL) was then dialyzed against buffer B at 4 °C and applied to a Mono Q HR 10/10 anion exchange column. The eluted fractions were pooled and concentrated by ultrafiltration to ~1 mM. A 2 mL aliquot of the concentrate was applied to a Superdex 75 gel filtration column equilibrated in buffer F [25 mM HEPES (pH 7.5), 100 mM KCl, 0.1 mM EDTA, and 1 mM DTT]. The collected fractions were combined and dialyzed against buffer S. Cleavage of the $His_6$ tag and the final purity were confirmed by SDS−PAGE. The concentration was determined with an extinction coefficient ($A_{280}$) of 10930 $cm^{-1}$ $M^{-1}$ for PEA-15.[27]

*Assay.* In vitro assays for tagless active ERK2 were performed in 100 μL volumes at 30 °C in buffer G [25 mM HEPES (pH 7.5), 50 mM KCl, 0.1 mM EDTA, 0.1 mM EGTA, 2 mM DTT, 10 mM $MgCl_2$, and 40 μg/mL BSA] containing 2 nM ERK2, 500 μM radiolabeled [$\gamma$-$^{32}$P]ATP (specific activity of 1 × $10^{15}$ cpm/mol), and 0−400 μM *Ets*. Reaction mixtures containing everything except ATP were prepared and kept on ice until the time of the assay. The reaction mixture was incubated for 10 min at 30 °C before the reaction was initiated with the radiolabeled ATP. Aliquots (10 μL) were spotted onto P81 filter papers at fixed times. The filter papers were each washed three times for 15 min with 50 mM phosphoric acid to remove excess ATP and washed once with acetone for drying. The amount of phosphate incorporated into *Ets* was determined by the associated counts per minute on a scintillation counter (Packard 1500) at a $\sigma$ value of 2.

**Light Scattering.** Active ERK2 (100−300 μM) was dialyzed against buffer F. Aliquots of $MgCl_2$ or $CaCl_2$ were then added from a 1 M stock solution to give concentrations of 0.5 or 10 mM prior to the light scattering experiments. PEA-15 (1000 μM) was also dialyzed against the same buffer without $MgCl_2$ or $CaCl_2$ prior to use. Light scattering analysis was performed on 100−300 μM active tagless ERK2 and 200 μM active $His_6$-tagged ERK2 in different experiments. The analysis of ERK2−PEA-15 association was conducted via injection of 20 μL of 300 μM active tagless ERK2 alone, 20 μL of 1 mM PEA-15 alone, and then 20 μL each of active tagless ERK2/PEA-15 mixtures (1:1 and 1:2 molar ratios) in which the ERK2 concentration was fixed at 300 μM to the size-exclusion column. Static light scattering measurements were taken as previously described[16,17] with the addition of dynamic light scattering with the Wyatt QELS detector (Wyatt Technology, Santa Barbara, CA). All measurements were taken at 25 °C. Size-exclusion chromatography was performed as previously described[16,17] with a TSK-GEL G3000$PW_{XL}$ column [300 mm × 7.8 mm (inside diameter), 14 mL column volume, Tosoh Bioscience LLC]. Buffer F, freshly prepared with Nanopure water (~18.3 MΩ cm) and filtered through a 0.02 μm filter (Anodisc 47, Whatman, catalog no. 6809-5002), was used to establish the light scattering and refractive index baselines. Bovine serum albumin monomer (Sigma A1900) was injected into the column at a concentration of 2 mg/mL for normalization of the light scattering detectors. Size-exclusion chromatography was conducted at a flow rate of 0.4 mL/min at room temperature with a run time of ~40 min. Samples were centrifuged for ~30 s to remove any insoluble components prior to injection. Molar masses, peak concentrations, and hydrodynamic radii were determined with Astra (Wyatt Technology).

**Analytical Ultracentrifugation.** Both sedimentation velocity and equilibrium experiments were conducted at 20 °C in a Beckman-Coulter Optima XL-I/A analytical ultracentrifuge with an AN60Ti rotor. The buffer used for all experiments contained 25 mM HEPES (pH 7.5), 100 mM KCl, 0.1 mM EDTA, 1 mM TCEP, with or without 10 mM $MgCl_2$, and various concentrations of tagless activated ERK2 as described below. Buffer densities were measured with an Anton Paar DMA 5000 density meter and found to be 1.0064 and 1.0057 $g/cm^3$ with and without 10 mM $MgCl_2$, respectively. Buffer viscosities calculated with SEDNTERP[28] were 1.023 and 1.019 cP with and without $MgCl_2$, respectively. A partial specific volume ($\bar{\nu}$) of ERK2 of 0.7403 $cm^3/g$ at 20 °C was calculated from the amino acid sequence with SEDNTERP.

Sedimentation equilibrium experiments were conducted with tagless active ERK2 loading concentrations of 4.8, 8.0, and 11.2 μM in six-sector Epon-charcoal centerpieces with quartz windows. Samples (110 μL) were spun at rotor speeds of 15000 and 25000 rpm until equilibrium was reached. Data were collected at 280 nm with 10 replicates with a step size of 0.001 cm. Data sets consisting of six curves were globally fit to various models using UltraScan version 9.9.[29] Sedimentation velocity experiments were conducted in double-sector Epon-charcoal centerpieces with quartz windows. The assembled cell was loaded with 430 μL of 15.2 μM tagless active ERK2 without $MgCl_2$ and allowed to equilibrate thermally with the rotor in the centrifuge chamber for a few hours. Scans were collected at 45000 rpm in continuous mode at 280 nm with 0.002 cm radial resolution and zero time intervals. Following this, 1.55 μL of $MgCl_2$ from a 2.8 M stock solution was added to the ERK2 sample in the assembled cell to give a final $MgCl_2$ concentration of 10 mM and tagless active ERK2 concentration of 15 μM. The cell was agitated to redistribute the sedimented protein and the sample run again. Data were analyzed by the enhanced van Holde−Weischet method[30] as incorporated in Ultrascan version 9.9. All sedimentation coefficient values are reported for water at 20 °C.

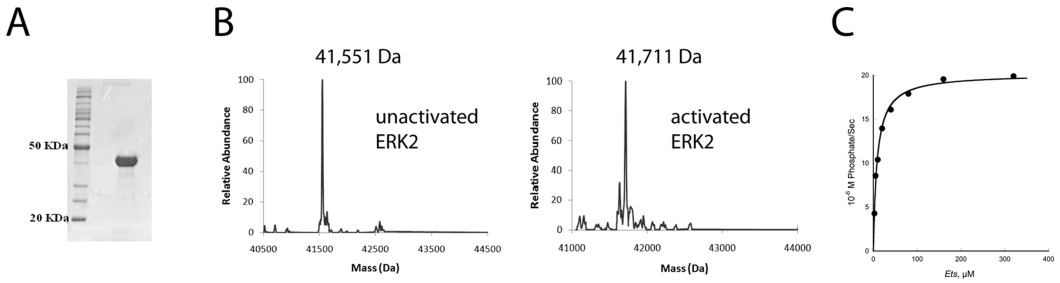


**Figure 1.** Purification of tagless ERK2. (A) Fractionation of tagless activated ERK2 by 10% SDS−PAGE. A BenchMark Protein Ladder (Invitrogen) is shown as a reference. (B) Mass spectrometry of thrombin-cleaved ERK2 (left, inactive form; right, fully active form). A constitutively active form of MKK1 was used to activate ERK2 by phosphorylation of two residues. (C) Phosphorylation of the substrate *Ets* by activated tagless ERK2 in the presence of 0.5 mM ATP and 10 mM $MgCl_2$.

**$^1$H NMR.** For $^1$H NMR experiments, we used a Bruker Avance spectrometer (operating at a nominal frequency of 600 MHz) at 298 K. NMR self-diffusion experiments were performed on tagless activated ERK2 in the absence or presence of 10 mM $MgCl_2$ in a buffer containing 10 mM sodium phosphate, 100 mM KCl, 0.5 mM EDTA, and 2 mM DTT. Lysozyme [1 mM in 30 mM NaCl (pH 2.8)] was used for calibration, and bovine serum albumin [0.65 mM in 10 mM sodium phosphate (pH 6.8)] was used as a standard. Diffusion coefficients were measured using a standard spin-echo and LED (longitude encode−decode) with bipolar encoding gradients,[31] two *z*-spoil gradients, and Watergate water suppression. Sixteen $^1$H spectra were acquired with 1024 scans, with a gradient strength increasing from 3.8 to 34.3 G/cm, three times. The encoding gradients were set to 4 ms, and the diffusion delay was 50 ms. The self-diffusion coefficient ($D_s$) is obtained from a fit of the signal decay to the relationship $I/I_o = \exp[-\gamma^2 G^2 \delta^2 (\Delta - \delta/3)/D_s]$, where $\gamma$ is the $^1$H gyromagnetic ratio, $\delta$ is the gradient duration (seconds), $G$ is the gradient strength (Gauss per centimeter), $\Delta$ is the time between PFG (pulse field gradient) pulses (seconds), and $I$ is the echo amplitude. Data were analyzed using Bruker Topspin version 1.3.

## RESULTS

Biophysical studies of the self-association of ERK2 have historically utilized a polypeptide containing six histidines inserted immediately between the initiating methionine and the first coding residue, Ala-2.[32] However, hexahistidine tags can promote self-association of some proteins,[20,21] so we constructed a new DNA expression plasmid encoding ERK2 to avoid this problem. The construct was designed such that cleavage by thrombin produces an ERK2 protein with just three residues, Gly-Ser-His, at the N-terminus before Met-1. Previously, we prepared activated $His_6$-ERK2 by utilizing a constitutive form of the upstream activator MKK1.[25] We used a mass spectrometry-based analysis of the undigested or tryptically digested protein to establish that MKK1 exclusively phosphorylates $His_6$-ERK2 at Thr-183 and Tyr-185 within the activation loop. Thrombin-cleaved ERK2 was prepared and activated as described above (Figure 1A,B) (see Materials and Methods). Mass spectrometry established that cleavage had occurred exclusively at the thrombin site and that the activated ERK2 contains two phosphates (Figure 1B). The tagless ERK2 was found to exhibit the same kinetic properties as $His_6$-ERK2. Initial velocity data at different concentrations of *Ets* were fitted with the Michaelis−Menten parameters [$k_{cat}$ = 19 $s^{-1}$, and $K_m$ = 8.5 $\mu$M (Figure 1C)], which matches what was established before for $His_6$-ERK2 by Waas et al.[33]

Measurement of the ability of tagless activated ERK2 to self-associate to a homodimer was conducted via gel filtration followed by light scattering (see Materials and Methods). The following buffer conditions were employed: 25 mM HEPES (pH 7.5), 100 mM KCl, 1 mM DTT, 0.1 mM EDTA, and 0, 0.5, or 10 mM $MgCl_2$ or $CaCl_2$ at 25 °C. The molar mass distribution, as a function of elution volume, is shown for each sample in Figure 2A−C. The concentrations of each of the central major peaks for the ∼7.2−8.8 mL range (determined at the peak maximum) were in the range of 0.4 mg/mL (∼9.0 $\mu$M) for the highest concentrations of ERK2 applied to the column. The weight-average molar mass of each of the central major peaks is ∼42 kDa, which is close to the sequence-derived mass of 41711 Da for activated ERK2 and therefore corresponds to the ERK2 monomer. The presence of either $MgCl_2$ or $CaCl_2$ up to 10 mM does not affect the weight-average molar mass of the monomer as ∼90−95% of the active ERK2 is monomeric (Figure 2A,B). Figure 2C also shows that in the absence of any divalent cations, activated ERK2 is ∼90−95% monomeric. We used dynamic light scattering [DLS or QELS (quasi-elastic light scattering)] to investigate further the self-association of ERK2. The translational diffusion coefficient, $D$, of a particle may be derived from dynamic light scattering measurements.[34,35] QELS was used to determine the translational diffusion coefficients for tagless active ERK2 applied to a gel filtration column at three concentrations (100, 200, or 300 $\mu$M) in the absence of metal ions and at 300 $\mu$M in the presence of 0.5 mM $MgCl_2$, 10 mM $MgCl_2$, 0.5 mM $CaCl_2$, and 10 mM $CaCl_2$. Analysis by Astra IV provides the hydrodynamic radius for the fractionated protein (indicated in Figure 2A−C). The average value over the major peak (∼7.2−8.8 mL) was used to determine the translational diffusion coefficient using the Stokes−Einstein equation.[36] In the presence and absence of free magnesium or calcium ions, the average diffusion coefficients determined by DLS were found to vary over the range of 8.36−8.59 × $10^{-7}$ $cm^2/s$. Thus, DLS confirms that the transitional diffusion coefficients of active tagless ERK2 are not affected by the presence of divalent cations or even by varying the concentration of ERK2. A small shoulder can be seen in the elution patterns for the monomeric ERK2 at ∼8.1 mL in Figure 2 but is not apparent in the ERK2 elution pattern in Figure 6. We interpret the main peak and shoulder to reflect different conformations of ERK2 molecules that do not differ significantly in molar mass. A very similar pattern has been observed by others,[16] who interpreted the main peak as a dimer

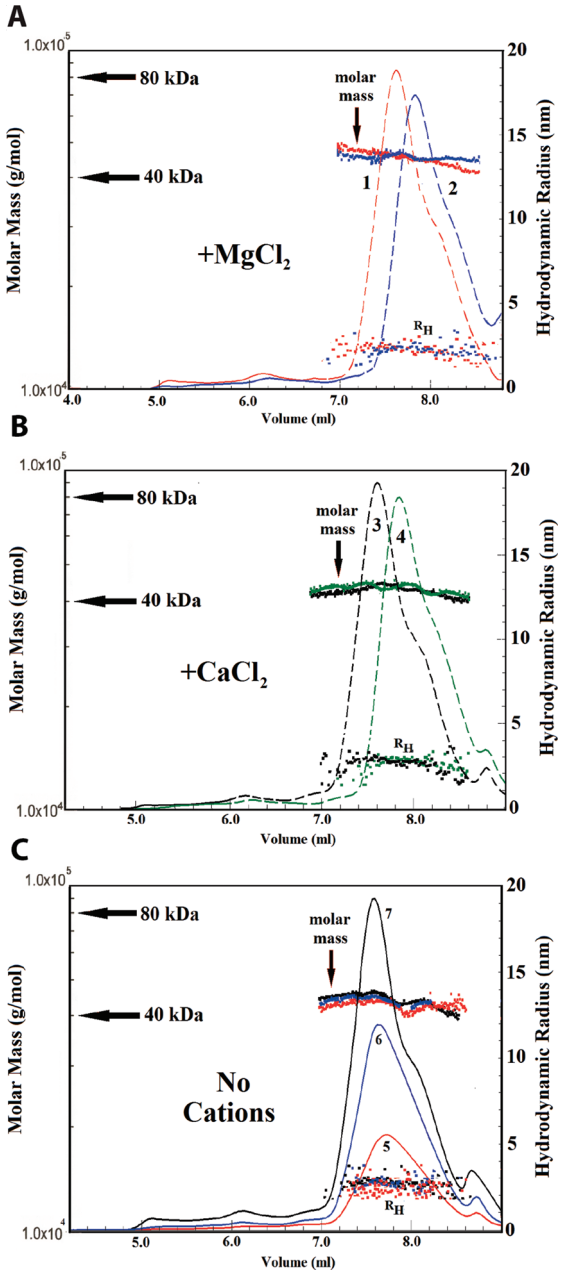


**Figure 2.** Light scattering analysis of active tagless ERK2 self-association. Fractionation of concentrated active ERK2 using size-exclusion chromatography followed by MALS-QELS analysis of ERK2 self-association. The chromatographic conditions are given in Materials and Methods. (A) Twenty microliters of 300 $\mu$M activated ERK2 with 0.5 mM $MgCl_2$ (1, red) and 20 $\mu$L of 300 $\mu$M activated ERK2 with 10 mM $MgCl_2$ (2, blue) were injected into the column and eluted at concentrations (at the maximum of each peak) of 5.4 and 5.1 $\mu$M, respectively. (B) Twenty microliters of 300 $\mu$M activated ERK2 with 0.5 mM $CaCl_2$ (3, black) and 20 $\mu$L of 300 $\mu$M activated ERK2 with 10 mM $CaCl_2$ (4, green) were injected into the column and eluted at concentrations (at the maximum of each peak) of 9 and 8.4 $\mu$M, respectively. (C) Twenty microliters of 100 $\mu$M (5, red), 200 $\mu$M (6, blue), and 300 $\mu$M (7, black) active ERK2 with no divalent cations were injected into the column and eluted at concentrations (at the maximum of each peak) of 1.5, 3.4, and 5.4 $\mu$M, respectively. The patterns represent the relative concentrations determined by measurement of the refractive index differences, the molar mass and Stokes radius ($R_H$), as a function of elution volume.

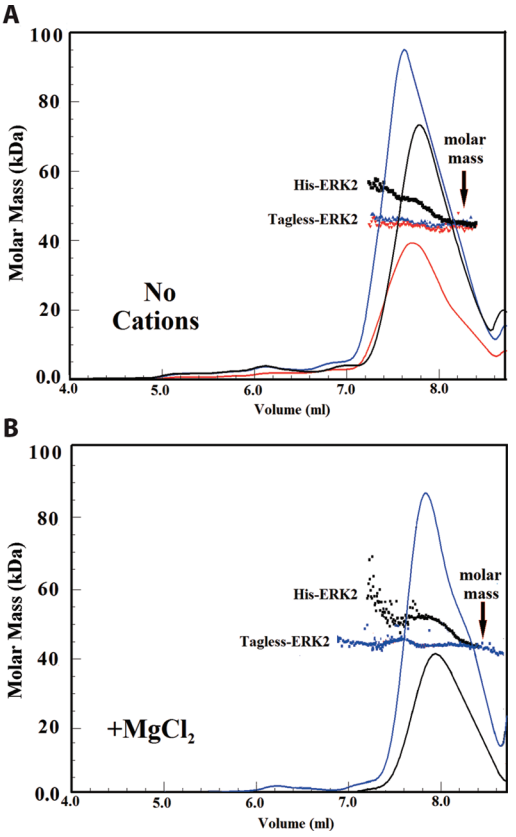


**Figure 3.** Light scattering analysis of the effect of the $His_6$ tag on the self-association of ERK2. Fractionation of active ERK2 with and without a $His_6$ tag shows that the $His_6$ tag on ERK2 causes significant dimerization. (A) Molar mass distribution in the absence of added divalent cations: black for 20 $\mu$L of ERK2 (200 $\mu$M) with the $His_6$ tag, red for 20 $\mu$L of ERK2 (100 $\mu$M) without the $His_6$ tag, and blue for 20 $\mu$L of ERK2 (200 $\mu$M) without the $His_6$ tag injected into the column and eluted at concentrations (at the maximum of each peak) of 2.7, 1.5, and 3.4 $\mu$M, respectively. (B) Molar mass distribution in the presence of 10 mM $MgCl_2$: black for 20 $\mu$L of ERK2 (200 $\mu$M) with the $His_6$ tag and blue for 20 $\mu$L of ERK2 (300 $\mu$M) without the $His_6$ tag injected into the column and eluted at concentrations (at the maximum of each peak) of 2.2 and 5.1 $\mu$M, respectively. The chromatographic conditions are the same as in Figure 2. All experiments were conducted in the presence of 0.1 mM EDTA.

and a shoulder as a monomer on the basis of the Stokes radius. Slightly different shapes or conformations can change the Stokes radius and modify the elution volume with no change at all in the molar mass.

Figure 3A compares ERK2 with and without a $His_6$ tag. The data show that the $His_6$ tag on ERK2 causes significant dimerization in the absence of added divalent cations. The apparent molar mass at ~7.4 mL, ~55 kDa, for the leading edge of the $His_6$-tagged ERK2 peak decreases to ~43 kDa at 8.4 mL. In the absence of the His tag, the molar mass does not change significantly across the elution peak. Figure 3B shows that the addition of $Mg^{2+}$ ions has no significant additional effect. The pattern for the His-tagged ERK2 in Figure 3A can be interpreted in terms of a monomer−dimer equilibrium. A weight-average molar mass of ~55 kDa corresponds to ~30% dimer. The size-exclusion column acts on a monomer to dimer equilibrium to separate dimer from monomer. However, as the dimer begins to

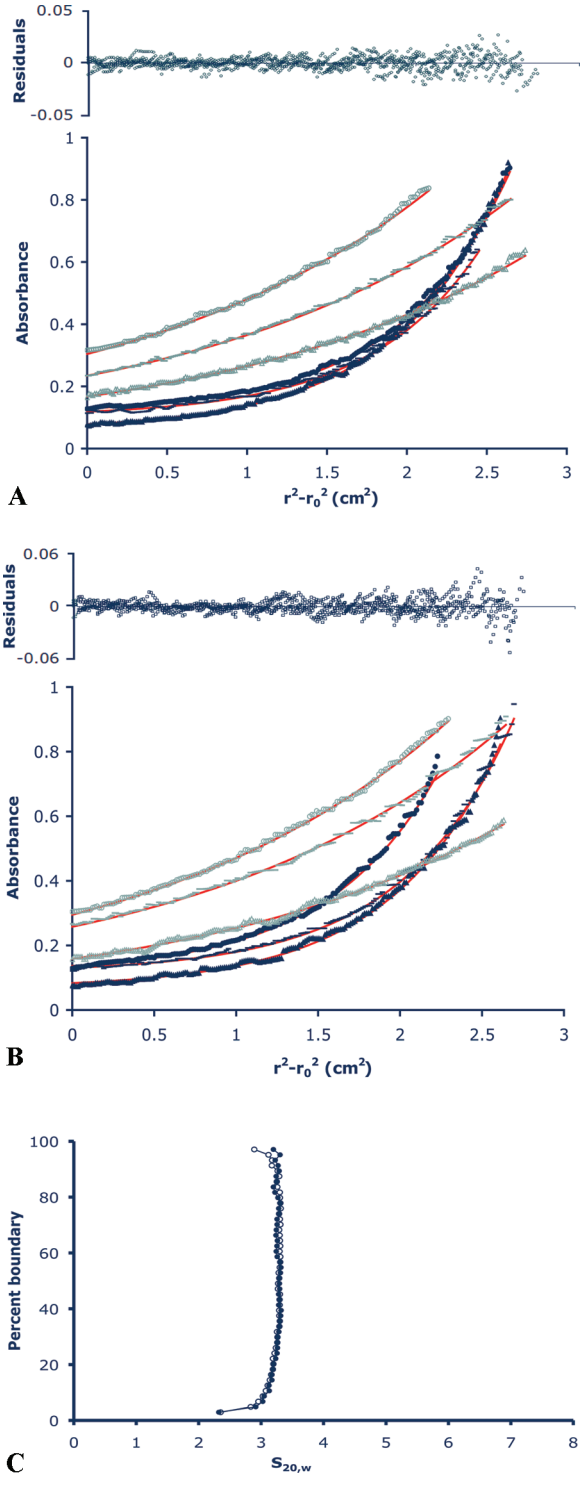


**Figure 4.** Sedimentation analysis of active tagless ERK2. In a volume of 110 $\mu$L, activated ERK2 at concentrations of 11.2 (1), 8 (2), and 4.8 $\mu$M (3) was spun at rotor speeds of either 15000 rpm (gray data points) or 25000 rpm (black data points) until equilibrium was achieved. The lines through the data correspond to the best fit to an ideal one-component system with the resulting residuals shown above the fits. Buffer contained (A) 0 mM $MgCl_2$ or (B) 10 mM $MgCl_2$. (C) Integral distribution plot showing an enhanced van Holde–Weischet analysis of velocity experiments of 15 $\mu$M activated ERK2 in the presence of either 0 (●) or 10 mM $MgCl_2$ (○). All sedimentation coefficient values are reported for water at 20 °C.

separate from the monomer, it starts to dissociate to reestablish equilibrium according to mass action requirements.

The experiments described here were conducted with the cleavable $His_6$ tagged ERK2 construct. Prior experiments with noncleavable $His_6$ tagged ERK2 are shown in Figure 6[a] of ref 17. These data show that ERK2 with the noncleavable $His_6$ tag is monomeric in contrast to our data for cleavable $His_6$-tagged ERK2 (Figure 3) that show that the cleavable $His_6$ tag allows ERK2 to dimerize. Thus, the nature of the $His_6$ tag adduct on ERK2 determines its effect on oligomerization.

We next examined the self-association of ERK2 by analytical ultracentrifugation. Sedimentation equilibrium experiments were performed using three different concentrations of tagless ERK2 (ranging from 4.8 to 11.2 $\mu$M) at two different rotor speeds in 25 mM HEPES (pH 7.5), 100 mM KCl, 0.1 mM EDTA, and 1 mM TCEP in the presence or absence of 10 mM $MgCl_2$. TCEP was used instead of DTT, because of the propensity of oxidized DTT to interfere with the detection of proteins at 280 nm. The sedimentation equilibrium data, over the range of concentrations, in the absence and presence of $MgCl_2$, were described well by an ideal one-component model with fitted molar masses of 40180 ± 480 and 41290 ± 660 Da, respectively (Figure 4A,B). This is consistent with the monomeric molar mass of ERK2 of 41711 Da. Analysis of the data using a monomer–dimer model failed to improve the fit and gives unreasonable dissociation constants of ~1 mM for an ERK2 dimer.

These results are supported by sedimentation velocity data obtained with a 15 $\mu$M solution of activated tagless ERK2. An enhancement[30] of the original method developed by van Holde and Weischet (vHW)[37] was adopted to determine the sedimentation coefficient of ERK2 in the absence and presence of 10 mM $MgCl_2$. The vHW method is particularly suited for distinguishing heterogeneous systems from single-component systems.[30] Notably, the integral distribution plots shown in Figure 4C, which are based on the enhanced vHW analysis, are virtually identical for the sample of ERK2 in the absence or presence of $MgCl_2$ and provide an average estimate of 3.2 S for the sedimentation coefficient of ERK2 in both solutions. Using the generally accepted hydrodynamic nonideality constant for globular proteins of 0.009 mL/mg, an ERK2 concentration of 0.63 mg/mL, and the experimentally determined $s_{20,w}$ of 3.2 S, the $s^0_{20,w}$ value at infinite dilution for ERK2 is calculated to be 3.22 S. The $s^0_{20,w}$ of 3.22 S ($f/f_0$ = 1.28) for the activated ERK2 monomer[b] is consistent with values determined for other globular proteins such as lysozyme ($M$ = 14400 Da) and serum albumin ($M$ = 66000 Da) that exhibit $s^0_{20,w}$ values of 1.91 ($f/f_0$ = 1.25) and 4.31 ($f/f_0$ = 1.35), respectively.[38] The molar mass, $M$, determined by sedimentation equilibrium and the sedimentation coefficient, $s$, may be used to estimate the translational diffusion coefficient $D$ for activated ERK2 using the Svedberg equation (eq 1).

$$\frac{s}{D} = \frac{M(1-\overline{\nu}\rho)}{RT}, \text{ which rearranges to } D = \frac{sRT}{M(1-\overline{\nu}\rho)} \quad (1)$$

Using an $R$ of 8.314 × $10^7$ g cm$^2$ s$^{-2}$ and a $T$ of 293 K, a $D_{20,w}$ value of 7.3 × $10^{-7}$ cm$^2$ s$^{-1}$ is obtained.[c] This compares to values of diffusion coefficients reported for lysozyme and bovine serum albumin at 20 °C of 11.2 × $10^{-7}$ and 5.94 × $10^{-7}$ cm$^2$ s$^{-1}$, respectively.[38] Taken together, the analytical ultracentrifugation

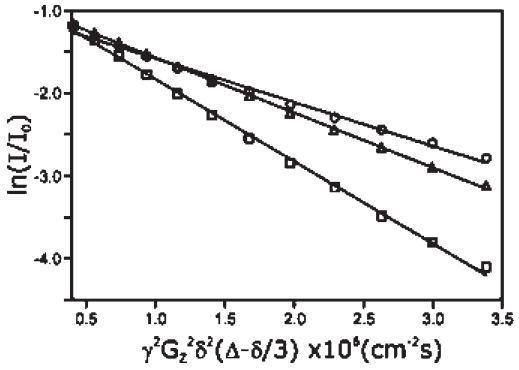


**Figure 5.** Translational diffusion attenuation of $^1$H NMR signal intensity for active tagless ERK2 in the absence of $MgCl_2$. The self-diffusion coefficient ($D_s$) is obtained from a fit of the signal decay to the relationship $I/I_o = \exp[-\gamma^2 G^2 \delta^2 (\Delta - \delta/3) D_s]$, where $G$ is the gradient strength (Gauss per centimeter) and $I$ is the echo amplitude. Logarithmic (normalized) signal intensities for activated ERK2 (△), bovine serum albumin (○), and lysozyme (□) from a single experiment.

and DLS experiments argue that phosphorylated ERK2 is monomeric in solution.

The rate of translational diffusion can be determined by $^1$H NMR from the signal decay that arises from molecular translation occurring during a diffusion delay period that is bracketed by defocusing and refocusing pulsed field gradients.[39] Thus, the translational diffusion coefficient of activated tagless ERK2 (55 $\mu$M) was determined using this bipolar pulse longitudinal eddy current delay approach in the absence or presence of 10 mM $MgCl_2$ in a buffer containing 10 mM sodium phosphate, 100 mM KCl, 0.5 mM EDTA, and 2 mM DTT at 25 °C. For comparison, diffusion experiments were also conducted with samples of 1 mM lysozyme and 0.65 mM BSA. The diffusion coefficients were obtained by fitting the decay of the protein $^1$H signal intensity as a function of defocusing or refocusing gradient strength as shown in Figure 5. The measured translational diffusion coefficient at 25 °C for activated ERK2 was determined to be $(8.7 \pm 0.4) \times 10^{-7}$ cm$^2$ s$^{-1}$ in the presence or absence of $MgCl_2$, and the translational diffusion coefficients for BSA and lysozyme were $(6.8 \pm 0.1)$ and $(12.9 \pm 0.1) \times 10^{-7}$ cm$^{-2}$ s$^{-1}$, respectively (Figure 5). These data demonstrate that activated tagless ERK2 diffuses faster than BSA (66 kDa) and slower than lysozyme (14.7 kDa) and support the notion that ERK2 is a monomer in solution at a concentration of 55 $\mu$M. The experimentally determined translational diffusion coefficient for ERK2 from NMR is in excellent agreement with the values calculated from the sedimentation and DLS experiments.

Although our light scattering, sedimentation, and NMR data show that ERK2 is monomeric, the possibility that accessory proteins might mediate the dimerization of ERK2 cannot be ignored. Cytoplasmic scaffolds have been reported to induce dimerization of ERK2.[40] We examined the possibility that ERK2 and the small cytoplasmic scaffold PEA-15[27] interact. We used the same approach described for the ERK2 self-association studies shown in Figure 2. Active ERK2 was applied to the column at a concentration of ~300 $\mu$M. As before, Figure 6A shows that the enzyme is predominantly monomeric at this high concentration in the absence of $MgCl_2$. On the basis of their amino acid compositions, the calculated molar masses of ERK2 and PEA-15 are 41717 and 15321 Da, respectively. Figure 6A shows that the much smaller PEA-15, ~15 kDa, elutes

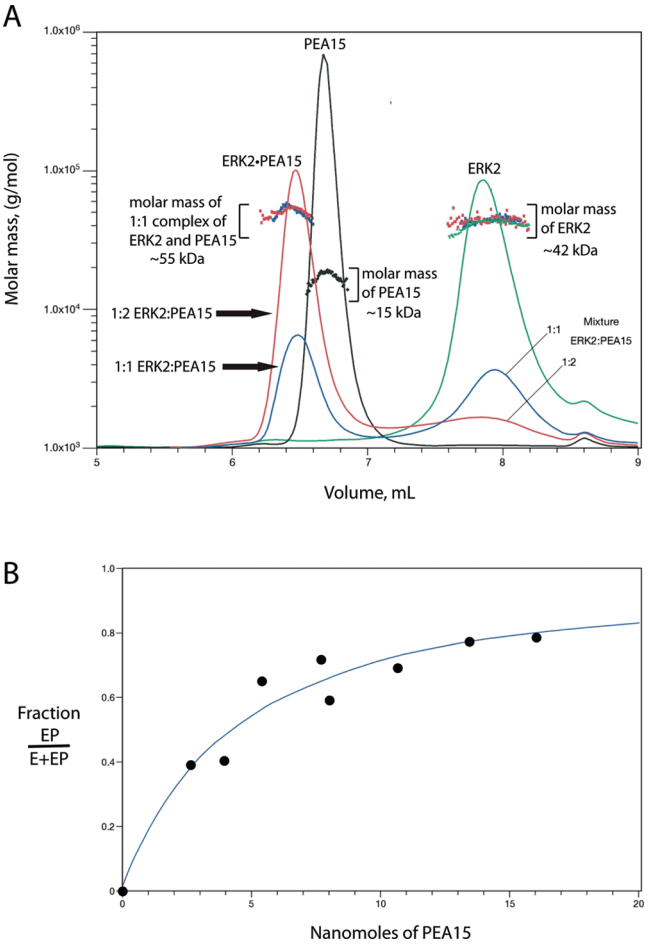


**Figure 6.** Light scattering analysis of an active tagless ERK2/PEA-15 mixture following fractionation with a size-exclusion column. (A) Four chromatograms are shown: active tagless ERK2 alone (~300 $\mu$M, green line), PEA-15 alone (~1 mM, black line), and two mixtures of ERK2 and PEA-15 at molar ratios of 1:1 (blue line) and 1:2 (red line) with the active tagless ERK2 concentration fixed at ~300 $\mu$M. The 1:1 molar ratio results in a complex with a measured molar mass of ~55 kDa (ERK2 monomer, 42 kDa, with PEA-15, 15 kDa, for a total of 57 kDa). The small peak at 8.6 mL is an artifact present in all samples. The solid lines represent the relative concentrations determined by measurement of the refractive indices. (B) Titration of active tagless ERK2 with PEA-15. ERK2 (4.35 nmol) was titrated with 0−16 nmol of PEA-15. The line corresponds to the best fit to an assumed $E + P \rightleftharpoons E \cdot P$ equilibrium. The concentrations seen by the refractometer are ~10-fold lower than those shown.

(~6.7 mL) from the size-exclusion column before the larger ERK2, ~42 kDa (~7.9 mL). This early elution reflects the extended conformation of PEA-15[41] and emphasizes that molar masses cannot be accurately determined solely from elution volumes. A mixture of ERK2 and PEA-15 results in the formation of a complex that elutes at ~6.4 mL with a molar mass of ~55 kDa as determined by MALS, close to the expected mass of 57 kDa for the E·P complex. This finding supports a 1:1 stoichiometry for the ERK2·PEA-15 complex (E·P).

A titration of ERK2 with PEA-15 was made by making mixtures with known compositions and subjecting them to MALS analysis after fractionation on the size-exclusion column. The quantity of the complex cannot be estimated directly because the peak for the complex overlaps with the elution of

free PEA-15 (Figure 6A). Measuring the concentration of free ERK2 and subtracting it from the known total amount of ERK2 in the composition of the initial mixture according to the relationship $[E \cdot P] = E_t - E_f$, where $E_t$ and $E_f$ are the total and free nanomoles of ERK2, respectively, allowed the amount of complex to be estimated. The fraction of ERK2 with bound PEA-15 was estimated from the ratio $(E_t - E_f)/E_t$. Figure 6B shows the titration of ERK2 with increasing amounts of PEA-15. The line corresponds to the best fit to an assumed $E + P \rightleftharpoons E \cdot P$ equilibrium. It should be noted that this is a titration and would represent a measure of a true equilibrium only if the rates of association and dissociation were extremely slow. The titration data support the stoichiometry of one molecule of PEA-15 forming a complex with one molecule of ERK2. The molar mass of the complex (~55000 Da) measured by MALS is close to the value expected for a 1:1 stoichiometry (57038 Da).

## DISCUSSION

**Activated ERK2 Is a Monomer in the Absence or Presence of Divalent Cations.** The purpose of this study was to evaluate the self-association of activated ERK2 in the presence or absence of divalent cations. X-ray crystallographic studies have revealed a potential interface for the stabilization of ERK2 homodimers by a nonhelical leucine zipper composed of L333, L334, and L336 from each monomer.[16] However, previous reports concerning the self-association of ERK2 in solution have been contradictory.[15−17] Activated $His_6$-ERK2 monomers were initially reported by Khokhlatchev et al.[15] to self-associate with high affinity (dissociation constant $K_d = 7$ nM) in the absence of added divalent metal ions. However, Wilsbacher et al.[16] and Callaway et al.[17] later reported that $His_6$-ERK2 is monomeric in the presence of chelating agents such as EDTA and EGTA. While dimerization was reported to be partially restored by the addition of divalent magnesium or calcium ions,[16] the possibility that trace transition metals promote dimerization of $His_6$-ERK2 in the absence of chelating agents, potentially through coordination to the $His_6$ tag, was not addressed. We have now assessed the possibility that activated tagless ERK2 might self-associate to form a homodimer. Activated ERK2 without the $His_6$ tag is fully active when assayed with the transcription factor substrate *Ets* (Figure 1).

Several complementary biophysical techniques were used to determine whether activated ERK2 forms specific homodimers (Figures 2−6). These techniques, taken together, provide a convincing description of activated ERK2 as a monomer in solution at concentrations 1 order of magnitude higher than the concentrations of 50−1000 nM normally found in mammalian cells.[42]

Gel filtration analysis of the eluted proteins by light scattering is a useful way to measure self-association.[43−45] Light scattering is necessary because elution volumes are very sensitive to conformation and ionic conditions and cannot be confidently used to determine accurate molar masses.[45,46] Light scattering is particularly helpful for characterizing polydisperse solutions of proteins that may result from significant aggregation. No significant self-association was observed in the presence of 0.5 or 10 mM free $Mg^{2+}$ or $Ca^{2+}$ ions (Figure 2A,B). Similarly, the monomeric fraction exceeded ~90% when ERK2 was loaded onto the SEC column at a concentration of 100, 200, or 300 $\mu$M in the absence of free divalent cations.[d] Moreover, QELS analysis indicates that the hydrodynamic radius $[R_{H(23,W)}]$ of ~2.8 nm for ERK2 is unaffected by the presence or absence of divalent cations (Figure 2A−C). This suggests that divalent cations do not affect ERK2 self-association at physiological or saturating concentrations.

Possible self-association of ERK2 was studied further via sedimentation equilibrium and velocity experiments, which are important approaches for examining the association of oligomers.[45,46] The longer experimental time scale of the sedimentation experiments makes possible the resolution of slowly equilibrating nonspecific aggregates.[45,46] Neither the sedimentation equilibrium nor the velocity experiments were able to detect any significant self-association of ERK2 either in the presence or in the absence of magnesium ions (Figure 4). The equilibrium experiments were fitted with a single species of ~42 kDa (Figure 4A,B). A sedimentation coefficient of ~3.22 S was calculated from the velocity data (Figure 4C). The frictional coefficient ratio $(f/f_0)$ was calculated to be 1.28 for monomeric activated ERK2, which lies in the range of 1.20−1.40 generally observed for globular proteins. The translational diffusion coefficient, $D$, was calculated to be $\sim 8.3 \times 10^{-7}$ cm$^2$ s$^{-1}$ for the activated ERK2 monomer. This finding was supported by dynamic light scattering, which also showed a translational diffusion coefficient $D$ of $\sim 8.3 \times 10^{-7}$ cm$^2$ s$^{-1}$ for ERK2 under all the experimental conditions. Furthermore, the NMR experiments showed a similar translational diffusion coefficient $D$ of $(8.7 \pm 0.4) \times 10^{-7}$ cm$^2$ s$^{-1}$ at 55 $\mu$M activated ERK2 (Figure 5). The excellent agreement between these three biophysical techniques in the determination of the translational diffusion coefficient confirms that phosphorylated ERK2 is monomeric in the presence or absence of divalent cations and at different ERK2 concentrations of 1.5−9 M.

**How Does ERK2 Associate with a Cytoplasmic Scaffold?** Studies of the self-association of ERK2 in vivo are contradictory. A FRET-based study failed to identify dimerization of activated GFP-ERK2 in cells.[18,e] A genetically encoded bioluminescence probe containing two ERK2 monomers joined by a linker was used as evidence of dimerization.[47] However, this latter approach is not a freely reversible process as the bioluminescence is dependent on the irreversible formation of *Renilla* luciferase and the monomers are present in the same polypeptide. Casar et al.[19] used the approach of Philipova and Whitaker[48] to report that ERK2 forms a homodimer on cytoplasmic scaffolds and substrates. They also report that only a monomer forms on nuclear substrates. We used static light scattering to examine the propensity of ERK2 to form a homodimer in association with the cytoplasmic scaffold PEA-15. Figure 6 clearly demonstrates that ERK2 and PEA-15 form a 1:1 complex of 57 kDa and that ERK2 is a monomer in this complex.

We have shown with three approaches that ERK2 has virtually no propensity to self-associate in the presence of physiological concentrations of either magnesium or calcium ions. Thus, if ERK2 forms dimers with cytoplasmic scaffolds, an underlying mechanism of selectivity must be associated with the process.

The method employed by Casar et al.,[19] which was first used by Philipova and Whitaker for the identification of ERK dimers in vivo,[48] requires incubation of the proteins under nonreducing conditions where they have a propensity to cross-link with disulfide bonds. As many mechanisms can bring two proteins to sufficiently close in space to form a chemical cross-link in a cellular lysate, such an approach can be misinterpreted. Most of the evidence supporting the importance of ERK2 homodimerization in solution utilizes the mutations originally identified by

Khokhlatchev et al.[15] These mutants were designed to break the putative homodimer interface seen in the crystal structure.[32] However, caution is needed when interpreting experiments with these mutants as their translocation to the nucleus (which is not dependent on dimerization) is impeded[40] and similar mutations in ERK1 render the protein unrecognizable by a phospho-specific antibody.[48] This suggests that the mutations may alter their ability to interact with other proteins.

## CONCLUSION

The ability of activated ERK2 to self-associate into specific homodimers at micromolar concentrations is not supported by a number of complementary biophysical techniques. Thus, ERK2 is unlikely to form specific homodimers in vivo at physiological concentrations. Although $His_6$-tagged ERK2 can form dimers under certain conditions, the tag is nonphysiological, so the dimers formed have no cellular significance. In addition, the assembly of activated ERK2 homodimers onto cytoplasmic scaffolds is not a general phenomenon. Further experimental work is required to establish whether such homodimers can form through cooperative interactions with scaffold proteins in vitro and in vivo.

## AUTHOR INFORMATION

### Corresponding Author

*Division of Medicinal Chemistry, College of Pharmacy, University of Texas, Austin, TX 78712. Telephone: (512) 471-9267. Fax: (512) 232-2606. E-mail: kinases@me.com.

### Notes

[a]The ordinate of Figure 6 in ref 17 is logarithmic and is labeled incorrectely. The label numbers 40, 50, and 60 should be changed to 10, 100, and 1000, respectively.

[b]If ERK2 behaves as a perfect unhydrated sphere sedimenting in pure water, the frictional coefficient, $f_0$, may be calculated from the relationship $f_0 = 6\pi\eta[(3M\bar{\nu})/(4\pi N_A)]^{1/3}$ using the following parameters: viscosity of water ($\eta$), $1.002 \times 10^{-2}$ P; molecular weight ($M$), 41290 (obtained from the sedimentation equilibrium experiment); partial specific volume of ERK2 ($\bar{\nu}$), 0.7403 mL/g; and Avogadro's number ($N_A$), $6.023 \times 10^{23}$ $mol^{-1}$. The actual frictional coefficient, $f$, for ERK2 undergoing sedimentation in water may be derived from the experimentally determined parameters using the relationship $f = \{[M(1 - \bar{\nu}\rho)]/(sN_A)\}$, where $\rho$ is the density of water (0.9982 g $mL^{-1}$), $s$ is the sedimentation coefficient at 20 °C in water determined by sedimentation velocity, and $M$ is the molecular weight determined by sedimentation equilibrium. Together, these calculations provide an estimate for the frictional coefficient ratio of activated ERK2 ($f/f_0$) of 1.28, which is as expected for globular proteins.

[c]This corresponds to a $D_{25,w}$ of $8.3 \times 10^{-7}$ $cm^2$ $s^{-1}$.

[d]A small amount of polydisperse material that elutes slightly earlier than the monomeric fraction may be observed when activated ERK2, which has been further purified by HIC, is applied to a SEC column at a concentration of ~300 $\mu$M in the absence of divalent metal ions.

[e]Lidke et al. (*J. Biol. Chem*, **2010**, *285*, 3092−3102) found no evidence for ERK1 dimerization in mouse embryo fibroblasts using fluorescence correlation spectroscopy.

### Author Contributions

T.S.K. and A.K.D. contributed equally to this work.

### Funding Sources

This research was supported in part by the grants from the Welch Foundation (F-1390) to K.N.D. and the National Institutes of Health to K.N.D. (GM59802). T.S.K. acknowledges a scholarship from the Egyptian Ministry of Higher Education. Light scattering instrumentation was funded by the National Science Foundation (Grant MCB-0237651 to A. F. Riggs).

## ACKNOWLEDGMENT

We acknowledge the excellent technical support from Claire Riggs. Analytical ultracentrifugation experiments were conducted in the Protein Analysis Facility of the Institute of Cell and Molecular Biology (ICMB) at the University of Texas. Mass spectra were recorded by Herng-Hsiang Lo in the CRED Analytical Instrumentation Facility Core at the University of Texas.

## ABBREVIATIONS

BSA, bovine serum albumin fraction V; DLS, dynamic light scattering; DTT, dithiothreitol; EDTA, ethylenediaminetetraacetic acid; EGTA, ethylene glycol bis(2-aminoethyl ether)-*N*,*N*,*N*′,*N*′-tetraacetic acid; ERK, extracellular signal-regulated protein kinase; ESI, electrospray ionization; ESI-MS, electrospray ionization mass spectrometry; *Ets*, murine $His_6$-tagged Ets-1 (1−138); FPLC, fast protein liquid chromatography; FRET, fluorescence resonance energy transfer; HEPES, *N*-(2-hydroxyethyl)piperazine-*N*′-2-ethanesulfonic acid; HIC, hydrophobic interaction column; IAA, iodoacetamide; IEG, immediate early genes; IPTG, isopropyl $\beta$-D-thiogalactopyranoside; JNK, c-Jun N-terminal kinase; MALS-QELS, multiangle quasi-elastic light scattering; MAPK, mitogen-activated protein kinase; MKK1, mitogen-activated protein kinase kinase 1; MKK6, mitogen-activated protein kinase kinase 6; PCR, polymerase chain reaction; PEA-15, astrocytic phosphoprotein; PKA, protein kinase A; PMSF, phenylmethanesulfonyl fluoride; SAP1/2, SRF accessory protein-1/2; SDS−PAGE, sodium dodecyl sulfate−polyacrylamide gel electrophoresis; TCEP, tris(2-carboxyethyl)phosphine hydrochloride; TFA, trifluoroacetic acid; TPCK, tosylphenylalanyl-chloromethane; TRIS, tris(hydroxymethyl)aminomethane.

## REFERENCES

(1) Chen, Z., Gibson, T. B., Robinson, F., Silvestro, L., Pearson, G., Xu, B., Wright, A., Vanderbilt, C., and Cobb, M. H. (2001) MAP kinases. *Chem. Rev. 101*, 2449–2476.

(2) Kaoud, T. S., Mitra, S., Lee, S., Taliaferro, J., Cantrell, M., Linse, K. D., Van Den Berg, C. L., and Dalby, K. N. (2011) Development of JNK2-Selective Peptide Inhibitors that Inhibit Breast Cancer Cell Migration. *ACS Chem. Biol. 6*, DOI: 10.1021/cb200017n.

(3) Blume-Jensen, P., and Hunter, T. (2001) Oncogenic kinase signalling. *Nature 411*, 355–365.

(4) Avruch, J., Zhang, X. F., and Kyriakis, J. M. (1994) Raf meets Ras: Completing the framework of a signal transduction pathway. *Trends Biochem. Sci. 19*, 279–283.

(5) Chong, H., Vikis, H. G., and Guan, K. L. (2003) Mechanisms of regulating the Raf kinase family. *Cell. Signalling 15*, 463–469.

(6) Schreck, R., and Rapp, U. R. (2006) Raf kinases: Oncogenesis and drug discovery. *Int. J. Cancer 119*, 2261–2271.

(7) Zheng, C. F., and Guan, K. L. (1993) Cloning and characterization of two distinct human extracellular signal-regulated kinase activator kinases, MEK1 and MEK2. *J. Biol. Chem. 268*, 11435–11439.

(8) Ferrell, J. E., Jr., and Bhatt, R. R. (1997) Mechanistic studies of the dual phosphorylation of mitogen-activated protein kinase. *J. Biol. Chem. 272*, 19008–19016.

(9) Brunet, A., Roux, D., Lenormand, P., Dowd, S., Keyse, S., and Pouyssegur, J. (1999) Nuclear translocation of p42/p44 mitogen-activated protein kinase is required for growth factor-induced gene expression and cell cycle entry. *EMBO J. 18*, 664–674.

(10) Chen, R. H., Chung, J., and Blenis, J. (1991) Regulation of pp90rsk phosphorylation and S6 phosphotransferase activity in Swiss 3T3 cells by growth factor-, phorbol ester-, and cyclic AMP-mediated signal transduction. *Mol. Cell. Biol. 11*, 1861–1867.

(11) Dalby, K. N., Morrice, N., Caudwell, F. B., Avruch, J., and Cohen, P. (1998) Identification of regulatory phosphorylation sites in mitogen-activated protein kinase (MAPK)-activated protein kinase-1a/p90rsk that are inducible by MAPK. *J. Biol. Chem. 273*, 1496–1505.

(12) Leighton, I. A., Dalby, K. N., Caudwell, F. B., Cohen, P. T., and Cohen, P. (1995) Comparison of the specificities of p70 S6 kinase and MAPKAP kinase-1 identifies a relatively specific substrate for p70 S6 kinase: The N-terminal kinase domain of MAPKAP kinase-1 is essential for peptide phosphorylation. *FEBS Lett. 375*, 289–293.

(13) Marais, R., Wynne, J., and Treisman, R. (1993) The SRF accessory protein Elk-1 contains a growth factor-regulated transcriptional activation domain. *Cell 73*, 381–393.

(14) Price, M. A., Rogers, A. E., and Treisman, R. (1995) Comparative analysis of the ternary complex factors Elk-1, SAP-1a and SAP-2 (ERP/NET). *EMBO J. 14*, 2589–2601.

(15) Khokhlatchev, A. V., Canagarajah, B., Wilsbacher, J., Robinson, M., Atkinson, M., Goldsmith, E., and Cobb, M. H. (1998) Phosphorylation of the MAP kinase ERK2 promotes its homodimerization and nuclear translocation. *Cell 93*, 605–615.

(16) Wilsbacher, J. L., Juang, Y. C., Khokhlatchev, A. V., Gallagher, E., Binns, D., Goldsmith, E. J., and Cobb, M. H. (2006) Characterization of mitogen-activated protein kinase (MAPK) dimers. *Biochemistry 45*, 13175–13182.

(17) Callaway, K. A., Rainey, M. A., Riggs, A. F., Abramczyk, O., and Dalby, K. N. (2006) Properties and regulation of a transiently assembled ERK2.Ets-1 signaling complex. *Biochemistry 45*, 13719–13733.

(18) Burack, W. R., and Shaw, A. S. (2005) Live Cell Imaging of ERK and MEK: Simple binding equilibrium explains the regulated nucleocytoplasmic distribution of ERK. *J. Biol. Chem. 280*, 3832–3837.

(19) Casar, B., Pinto, A., and Crespo, P. (2008) Essential role of ERK dimers in the activation of cytoplasmic but not nuclear substrates by ERK-scaffold complexes. *Mol. Cell 31*, 708–721.

(20) Wu, J., and Filutowicz, M. (1999) Hexahistidine (His6)-tag dependent protein dimerization: A cautionary tale. *Acta Biochim. Pol. 46*, 591–599.

(21) Amor-Mahjoub, M., Suppini, J. P., Gomez-Vrielyunck, N., and Ladjimi, M. (2006) The effect of the hexahistidine-tag in the oligomerization of HSC70 constructs. *J. Chromatogr., B: Anal. Technol. Biomed. Life Sci. 844*, 328–334.

(22) Szafranska, A. E., Luo, X., and Dalby, K. N. (2005) Following in vitro activation of mitogen-activated protein kinases by mass spectrometry and tryptic peptide analysis: Purifying fully activated p38 mitogen-activated protein kinase α. *Anal. Biochem. 336*, 1–10.

(23) Ueda, E. K., Gout, P. W., and Morganti, L. (2003) Current and prospective applications of metal ion-protein binding. *J. Chromatogr., A 988*, 1–23.

(24) Abramczyk, O., Rainey, M. A., Barnes, R., Martin, L., and Dalby, K. N. (2007) Expanding the repertoire of an ERK2 recruitment site: Cysteine footprinting identifies the D-recruitment site as a mediator of Ets-1 binding. *Biochemistry 46*, 9174–9186.

(25) Waas, W. F., Rainey, M. A., Szafranska, A. E., and Dalby, K. N. (2003) Two rate-limiting steps in the kinetic mechanism of the serine/threonine specific protein kinase ERK2: A case of fast phosphorylation followed by fast product release. *Biochemistry 42*, 12273–12286.

(26) Callaway, K., Rainey, M. A., and Dalby, K. N. (2005) Quantifying ERK2-protein interactions by fluorescence anisotropy: PEA-15 inhibits ERK2 by blocking the binding of DEJL domains. *Biochim. Biophys. Acta 1754*, 316–323.

(27) Callaway, K., Abramczyk, O., Martin, L., and Dalby, K. N. (2007) The anti-apoptotic protein PEA-15 is a tight binding inhibitor of ERK1 and ERK2, which blocks docking interactions at the D-recruitment site. *Biochemistry 46*, 9187–9198.

(28) Laue, T. M., Shah, B. D., Ridgeway, T. M., and Pelletier, S. L. (1992) Computer-aided Interpretation of Anaytical Sedimentation Data for Proteins. In *Analytical Ultracentrifugation in Biochemistry and Polymer Science* (Harding, S. E., Rowe, A. J., and Horton, J. C., Eds.) pp 90−125, Royal Society of Chemistry, Cambridge, U.K.

(29) Demeler, D. (2005) UltraScan: A comprehensive data analysis software for analytical ultracentrifugation experiments. In *Analytical ultracentrifugation: Techniques and methods* (Scott, D. J., Harding, S. E., and Rowe, A. J., Eds.) pp 210−229, Royal Society of Chemistry, Cambridge, U.K.

(30) Demeler, B., and van Holde, K. E. (2004) Sedimentation velocity analysis of highly heterogeneous systems. *Anal. Biochem. 335*, 279–288.

(31) Wu, D., Chen, A., and Johnson, C. S., Jr. (1995) An improved diffusion-ordered spectroscopy experiment incorporating bipolar-gradient pulses. *J. Magn. Reson., Ser. A 115*, 260–264.

(32) Canagarajah, B. J., Khokhlatchev, A., Cobb, M. H., and Goldsmith, E. J. (1997) Activation mechanism of the MAP kinase ERK2 by dual phosphorylation. *Cell 90*, 859–869.

(33) Waas, W. F., and Dalby, K. N. (2001) Purification of a model substrate for transcription factor phosphorylation by ERK2. *Protein Expression Purif. 23*, 191–197.

(34) De Jaeger, N., Demeyere, H., Finsy, R., Sneyders, R., van der Meeren, P., and van Laethem, M. (1991) Particle Sizing by Photon Correlation Sectroscopy Part I: Monodisperse latices: Influence of scattering angle and concentration of dispersed material. *Part. Part. Syst. Charact. 8*, 179–186.

(35) Burchard, W. (1996) Combined Static and Dynamic Light Scattering. In *Light scattering: Principles and development* (Brown, W., Ed.) pp 439−476, Clarendon, Oxford, U.K.

(36) Will, S., and Leipertz, A. (1997) Measurement of particle diffusion coefficients with high accuracy by dynamic light scattering. *Prog. Colloid Polym. Sci. 104*, 110–112.

(37) Van Holde, K. E., and Weischet, W. O. (1978) Boundary analysis of sedimentation velocity experiments with monodisperse and paucidisperse solutes. *Biopolymers 17*, 1387–1403.

(38) Van Holde, K. E., Johnson, W. C., and Ho, P. S. (2006) *Principles of physical biochemistry*, International Edition, 2nd ed., Pearson/Prentice Hall, Upper Saddle River, NJ.

(39) Garcia de la Torre, J., Huertas, M. L., and Carrasco, B. (2000) HYDRONMR: Prediction of NMR relaxation of globular proteins from atomic-level structures and hydrodynamic calculations. *J. Magn. Reson. 147*, 138–146.

(40) Casar, B., Arozarena, I., Sanz-Moreno, V., Pinto, A., Agudo-Ibanez, L., Marais, R., Lewis, R. E., Berciano, M. T., and Crespo, P. (2009) Ras subcellular localization defines extracellular signal-regulated kinase 1 and 2 substrate specificity through distinct utilization of scaffold proteins. *Mol. Cell. Biol. 29*, 1338–1353.

(41) Farina, B., Pirone, L., Russo, L., Viparelli, F., Doti, N., Pedone, C., Pedone, E. M., and Fattorusso, R. (2010) NMR backbone dynamics studies of human PED/PEA-15 outline protein functional sites. *FEBS J. 277*, 4229–4240.

(42) Huang, C. Y., and Ferrell, J. E., Jr. (1996) Ultrasensitivity in the mitogen-activated protein kinase cascade. *Proc. Natl. Acad. Sci. U.S.A. 93*, 10078–10083.

(43) Folta-Stogniew, E., and Williams, K. R. (1999) Determination of molecular masses of proteins in solution: Implementation of an HPLC size exclusion chromatography and laser light scattering service in a core laboratory. *J. Biomol. Tech. 10*, 51–63.

(44) Winzor, D. J. (2003) Analytical exclusion chromatography. *J. Biochem. Biophys. Methods 56*, 15–52.

(45) Philo, J. S. (2006) Is any measurement method optimal for all aggregate sizes and types?. *AAPS J. 8*, E564–E571.

(46) Lebowitz, J., Lewis, M. S., and Schuck, P. (2002) Modern analytical ultracentrifugation in protein science: A tutorial review. *Protein Sci. 11*, 2067–2079.

(47) Kaihara, A., and Umezawa, Y. (2008) Genetically encoded bioluminescent indicator for ERK2 dimer in living cells. *Chem.—Asian J. 3*, 38–45.

(48) Philipova, R., and Whitaker, M. (2005) Active ERK1 is dimerized in vivo: Bisphosphodimers generate peak kinase activity and monophosphodimers maintain basal ERK1 activity. *J. Cell Sci. 118*, 5767–5776.